

# High-Temperature Homopolymerization of Ethyl Acrylate and *n*-Butyl Acrylate: Polymer Characterization

Congling Quan and Masoud Soroush\*

Department of Chemical and Biological Engineering, Drexel University,  
Philadelphia, Pennsylvania 19104

Michael C. Grady and Joan E. Hansen

Marshall Laboratory, E.I. duPont de Nemours and Company, Philadelphia, Pennsylvania 19146

William J. Simonsick, Jr.

Stine-Haskell Research Center, E.I. duPont de Nemours and Company, 1090 Elkton Road,  
Newark, Delaware 19711

Received December 1, 2004; Revised Manuscript Received June 16, 2005

**ABSTRACT:** This paper presents a thorough molecular characterization of ethyl acrylate (EA) and *n*-butyl acrylate (nBA) homopolymers made at high temperature (140–180 °C) to high conversions (50–90%) in xylene isomers without the use of added thermal initiator. Electrospray ionization/Fourier transform mass spectrometry (ESI/FTMS) analysis shows four dominant chain types formed during high-temperature polymerization. Chains initiated by  $\beta$ -scission radicals and by xylol radicals that grow and eventually terminate to form terminally saturated and unsaturated chains. These chain structures suggest the underlying secondary mechanisms in high-temperature acrylate polymerization include  $\beta$ -scission (disproportionation) of the carbon-centered tertiary radical that is most likely formed via intramolecular chain transfer. Additionally, chain transfer to solvent, xylene in this case, also plays an important mechanistic role. Results from 1D NMR using  $^{13}\text{C}$ ,  $^1\text{H}$ , and distortionless enhancement polarization transfer (DEPT) corroborate the ESI/FTMS results and additionally predict (i) 2 branch points per chain on average for EA homopolymer with a number-average molecular weight of 4000 and (ii) 1.25 branch points per chain on average for nBA homopolymer with a number-average molecular weight of 3300. The presence of branch points indicates propagation of the midchain tertiary radical does occur to significant extent under the conditions of the experiments. Neither the ESI/FTMS nor NMR results suggest a mechanistic route by which the acrylates initiate polymerization without added thermal initiator.

## 1. Introduction

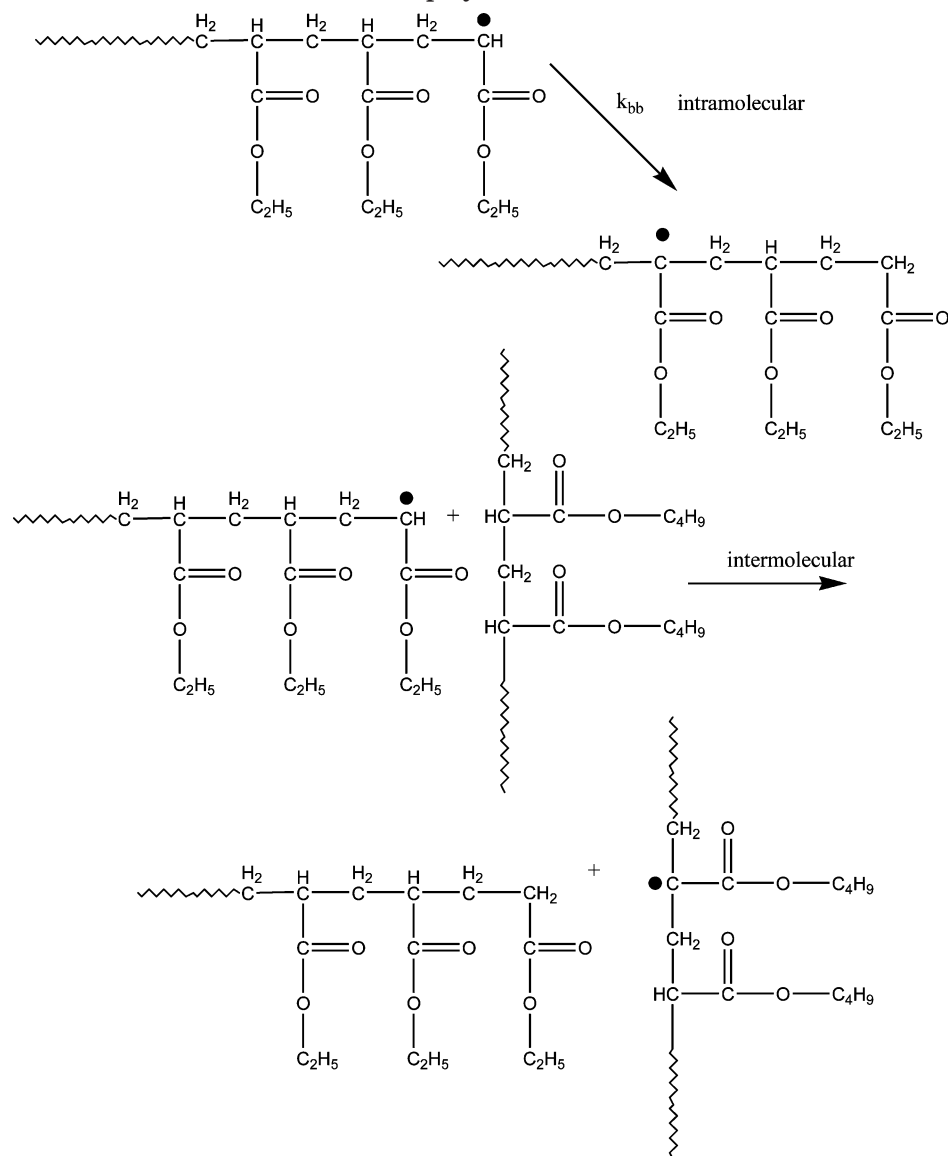
Secondary reactions in solution free-radical acrylic polymerization become important at high temperatures and strongly influence the nature of the polymer formed.<sup>1</sup> A fundamental understanding of the influence of the various secondary reaction mechanisms is valuable for both designing and optimizing the high-temperature polymerization processes and their products.<sup>2–5</sup>

High-temperature polymerizations of styrene and ethylene are well studied. Styrene is known to thermally polymerize<sup>6,7</sup> and ethylene to form branched polymer chains.<sup>8</sup> More recently, short chain branching in alkyl acrylates and depropagation in alkyl methacrylates have been studied and identified as principal secondary reactions in higher temperature free-radical acrylic polymerization.<sup>9</sup> These reactions behave as molecular weight and functional group placement regulators.<sup>10</sup> For the alkyl acrylates, the secondary mechanisms are thought to be responsible for (i) the wide disparity in reported values of the propagation and termination rate constants,  $k_p$  and  $k_t$ ; (ii) the discrepancy between (a) the pulsed-laser polymerization values of  $k_p$  values determined at temperatures greater than 35 °C and (b) the extrapolated values of  $k_p$  values obtained through low-temperature (below 25 °C) pulsed-laser polymerization experiments;<sup>11,12</sup> and (iii) the measured monomer reac-

tion orders of 1.5 and greater (unity is expected) for alkyl acrylate polymerizations.<sup>13–16</sup>

One interpretation of these anomalies in the kinetic values is the facile formation of a tertiary carbon-centered radical formed by hydrogen abstraction from the methine group on the main chain, namely an intramolecular chain transfer reaction described as intramolecular backbiting and shown in Scheme 1. The tertiary radical formed is slow to propagate and terminate,<sup>17</sup> causing the discrepancies in  $k_p$  and  $k_t$  values. Others have shown, through electron spin resonance (ESR) of the propagating radical of phenyl acrylate<sup>18</sup> and cyclohexyl acrylate,<sup>19</sup> the presence of two radical species: the secondary radicals at chain end and less active tertiary chain-centered radicals. The latter are present at even low monomer conversion, having led many to hypothesize the intramolecular chain transfer mechanism and to predict its dominance under dilute polymer conditions.<sup>20</sup> However, ESR cannot distinguish a tertiary radical formed by intermolecular chain transfer (hydrogen abstraction from a polymer chain by a separate polymer radical and also shown in Scheme 1) from that formed by intramolecular chain transfer.  $^{13}\text{C}$  NMR studies of nBA homopolymerization show the existence of a branching point by quaternary carbon resonance at a chemical shift ( $\delta_{\text{C}}$ ) of about 48 ppm.<sup>21–25</sup> But as with ESR, neither  $^{13}\text{C}$  NMR,  $^1\text{H}$  NMR, nor electrospray ionization/Fourier transform spectroscopy (ESI/FTMS) analysis of the formed polymer chains can distinguish the nature of the mechanism by which the

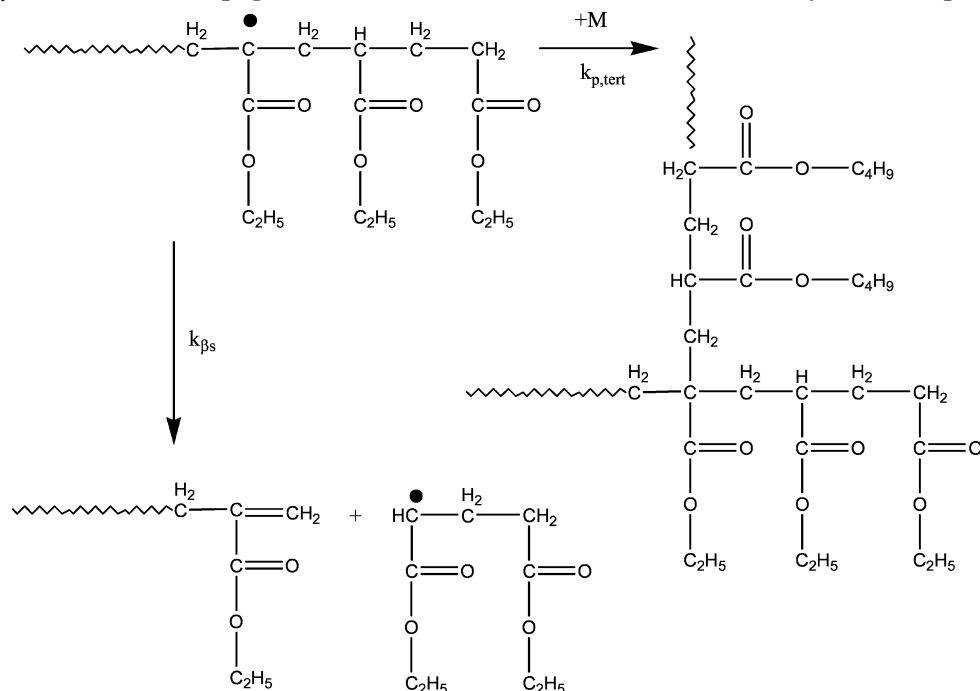
\* Corresponding author: Tel (215)-895-1710, Fax (215)-895-5837, e-mail masoud.soroush@drexel.edu.

**Scheme 1. Intramolecular (Top) and Intermolecular Routes to Midchain Tertiary Radicals in Acrylate Homopolymerization**

carbon-centered radical is formed. Many believe that intermolecular hydrogen abstraction is significant under concentrated polymer conditions. A broadening of the polydispersity of the molecular weight distribution is expected when intermolecular chain transfer is present. Asua et al.<sup>19</sup> and Lovell et al.<sup>18</sup> investigated emulsion polymerization of nBA at lower temperatures (i.e., highly concentrated polymer conditions) under starved feed conditions and differed in their conclusions regarding the dominant reaction mechanism. Under the conditions of this study, relatively low monomer concentration and high temperatures, intramolecular chain transfer is expected to be significant. Irrespective of the formation mechanism, the formed carbon-centered radical, especially at higher temperatures,<sup>16</sup> undergoes  $\beta$ -scission to generate a  $\beta$ -scission radical and terminally unsaturated macromonomer, as shown in Scheme 2. The carbon-centered tertiary radical can also undergo any of the common radical reactions including propagation (shown in Scheme 2), chain transfer to solvent, to monomer, or to polymer and termination with other radicals. Both the  $\beta$ -scission and propagation reactions lead to re-formation of the secondary chain-end radical. The  $\beta$ -scission radical and macromonomer formed have

unique molecular weights owing to the nature of the decomposition. The radical surrenders a  $\text{CH}_2$  to form the macromonomer. The resulting macromonomer has a molecular weight 14 Da greater than a chain comprised of polymerized acrylate monomer units while the  $\beta$ -scission radical has a molecular weight 14 Da less than a chain of acrylate monomer units. These unique molecular weight signals make ESI/FTMS ideally suited for detecting the presence of mechanistic steps involving macromonomer and  $\beta$ -scission radicals.

In this paper, nBA and EA homopolymers, produced at high temperatures (140–180 °C) in xylene isomers without the use of traditional free-radical initiators and at different monomer concentrations (10 and 40 wt % on solution), are characterized by ESI/FTMS and 1D  $^{13}\text{C}$  and  $^1\text{H}$  NMR in order to determine the extent of the secondary reactions involved in the polymerization. Significant to this work is the lack of added thermal initiator, and the lack of identifiable initiator end groups on the polymer chains, as an indication of the propensity of alkyl acrylates to undergo spontaneous polymerization and as a way to examine these secondary reactions without initiator end groups present.

Scheme 2.  $\beta$ -Scission and Propagation of the Midchain Radicals Formed in Acrylate Homopolymerization

The organization of this paper is as follows. Section 2 describes the experimental setup and procedures as well as the analytical instruments employed for these studies. Section 3 presents a discussion of the results. Finally, section 4 provides some concluding remarks.

## 2. Experimental Section

**2.1. Polymerization.** EA and nBA (BASF, 99.5%) were purified by passing monomers through an inhibitor removal column (DHR-4, Scientific Polymer Products, Inc.). Xylene (ExxonMobil Chemical Co, an 80/20 mix of xylene isomers and ethylbenzene with a boiling point range of 137–143 °C) and 4-methoxyphenol (99%, ACROS) were used as received. The polymerizations were carried out in a 1 L RC1 calorimeter (Mettler-Toledo GmbH, Schwerzenbach, Switzerland). The process employed started with purging nitrogen gas through the empty reactor and the raw materials in the feed tank for 30 min. The monomer and solvent were then pumped from the feed tank to the reactor and heated under a nitrogen blanket to reaction temperature. Reaction temperature was maintained throughout the course of the polymerization by adjustment of the reactor jacket temperature. Samples were drawn from the reaction at specified times and diluted 50/50 v/v in a cold 1000 ppm 4-methoxyphenol inhibitor solution to stop further reaction. Polymer content was determined by gravimetry. Molecular weight distributions were determined using a Hewlett-Packard (Palo Alto, CA) 1090 high-performance liquid chromatograph equipped with a Hewlett-Packard 1047A refractive index detector. The column set employed for the studies was a four-column set consisting of  $10^5$ ,  $10^4$ ,  $10^3$ , and  $10^2$  Å 30 cm  $\times$  7.8 mm i.d. Microstyragel columns (Waters, Milford, MA). Tetrahydrofuran (THF) at 40 °C was used as the mobile phase at a flow of 1 mL/min. Data from the RI detector were collected and processed using a Waters Millennium system. Narrow molecular weight polystyrene (PS) standards were used to calibrate the column set. The PS calibration provided reasonable accuracy for the low-molecular-weight nBA and EA homopolymers produced in this study.<sup>9</sup>

**2.2. Electrospray Ionization Mass Spectroscopy.** The direct electrospray experiments were conducted on a Finnigan FTMS Newstar system equipped with an Ultra-Source II electrospray ionization source assembly (Madison, WI). The pEA and pBA samples were dissolved in tetrahydrofuran (THF) to a concentration of  $\sim 50$  mg/mL. Sodium iodide was

Table 1. nBA Homopolymerization Results

<i>T</i> (°C)	wt fraction of nBA on formula	<i>M<sub>w</sub></i>	<i>M<sub>n</sub></i>	<i>M<sub>w</sub>/M<sub>n</sub></i>	% conv of nBA	time (min) to achieve conv
140	40	21863	9886	2.2	72	188
160	10	2411	1895	1.3	37	142
160	20	4076	2700	1.5	70	170
160	40	10555	5104	2.1	80	166
160	40	10642	5177	2.1	83	170
180	40	7102	3308	2.1	88	137

added to the THF solution to a concentration of  $\sim 100$   $\mu$ M. The capillary voltage was set to 3 keV for all experiments.

For each spectrum, ions were accumulated in the analyzer cell for 1 s with the trap plates at 6.5 V and a pulse argon gas pressure of  $10^{-6}$  Torr. After a 3.5 s delay (trap plates held at 2 V) to allow the pressure to be pumped down to  $5 \times 10^{-8}$  Torr, any ions below 240 *m/z* were ejected using a chirp excitation. Following an additional delay of 0.05 s the remaining ions were excited (chirp) and detected with trap plates at 0.5 V. Each acquisition contained 128K data points with a lower mass limit of 300 *m/z*. Twenty spectra were summed, and one zero fill was performed.

**2.3. NMR Spectroscopy.** Samples for NMR spectroscopy were isolated from the quenched polymerization mixtures by evaporation at 65 °C and high vacuum. NMR spectra were recorded at 34 °C on a Bruker DRX-400 MHz spectrometer (<sup>1</sup>H frequency of 400.13 MHz and <sup>13</sup>C frequency of 100.61 MHz). Deuterated chloroform (CDCl<sub>3</sub>) was used as solvent for all experiments. 1D <sup>13</sup>C and DEPT spectra were collected using a 10 mm broadband probe equipped with <sup>1</sup>H decoupling. <sup>1</sup>H NMR spectra were recorded using a 9.1 s acquisition time, a 3.6 kHz spectral window, a 30 s relaxation time, and an 88  $\mu$ s 90° <sup>1</sup>H pulse. For <sup>13</sup>C NMR spectra the values were 1.36 s acquisition time, a 24 kHz spectral window, a 30 s relaxation time, and a 14  $\mu$ s 90° <sup>13</sup>C pulse. The DEPT spectra were collected under similar conditions, except for a 5 s relaxation time and a 23  $\mu$ s 90° <sup>1</sup>H pulse.

## 3. Results and Discussion

Table 1 contains the results of the nBA polymerization experiments. Monomer conversion increases with temperature at a given monomer content and with monomer content at a given temperature. The conver-

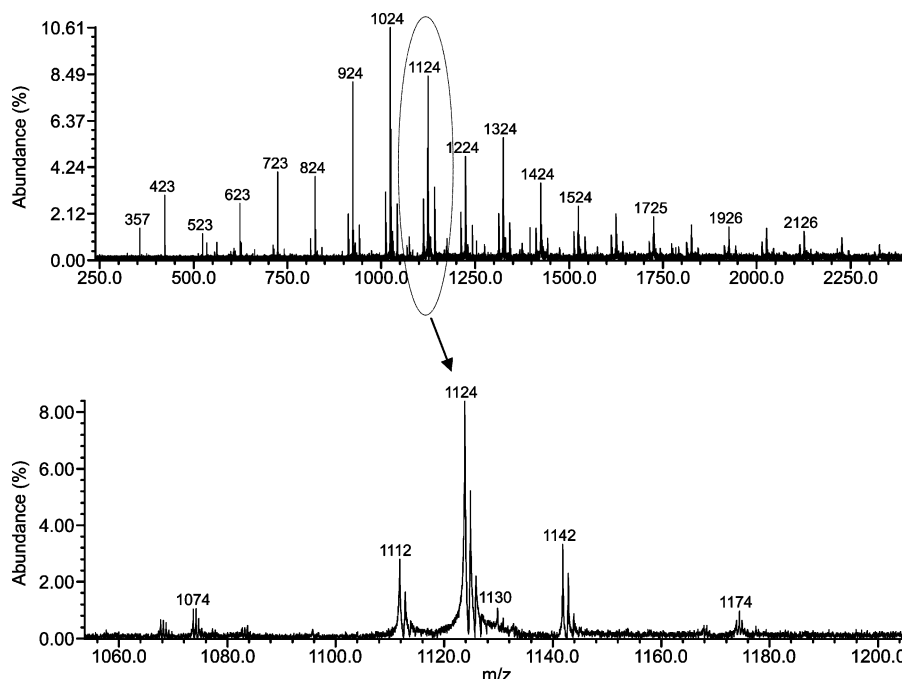


**Figure 1.** ESI/FTMS spectra of poly(ethyl acrylate) sample made by spontaneous polymerization at 180 °C and 40 wt % monomer on solution in the range between 250 and 2250 Da. Also shown is the expanded view of ESI/FTMS results around the peak 1124 Da. The expanded range is 1060–1200 Da.

sion data compare reasonably with those of Chiefari et al.<sup>20</sup> for initiated homopolymerization of nBA. In their work, Chiefari et al. used a very small amount of higher temperature azo-initiator and on comparison with this work may have been measuring some fraction of the nBA conversion due to spontaneous polymerization. Many such alkyl acrylates undergo spontaneous thermal polymerization as noted in Grady et al.<sup>26</sup> The mechanism by which the alkyl acrylates undergo spontaneous polymerization is not known, and a mechanism by which they might spontaneously polymerize is not obvious. Acrylates and methacrylates do not have the chemical structure necessary to undergo the Diels–Alder reaction that is the source of styrene spontaneous polymerization.<sup>3</sup> Without an obvious mechanism, spontaneous polymerization of alkyl acrylates has been attributed to impurities in the reaction mass, e.g., peroxides formed by oxidized monomer or even dissolved molecular oxygen.<sup>27</sup> The sustainability of the polymerization, over hours and not minutes, is of interest especially if impurities are the root cause.

### 3.1. Chain Composition Analysis by ESI/FTMS.

The low-molecular-weight nBA and EA homopolymers made via spontaneous initiation were analyzed using ESI/FTMS as described in the Experimental Section. We have found that the upper limit on molecular weight analyzed by direct ESI/FTMS, as practiced in our laboratory, is ~2500 Da, and this represents a significant portion of the overall distribution in the samples analyzed. We have been able to analyze chains with molecular weights in excess of 10K Da, although a GPC was required prior to ESI/FTMS analysis.<sup>28</sup> For the lowest molecular weight nBA sample, with  $M_w = 2800$ , the ESI/FTMS looks at over 70% of the weight fraction of the chains within the molecular weight distribution. As such, the end groups identified within the ESI/FTMS represent the majority of the end groups formed over the course of the polymerization. For the highest molecular weight sample, with  $M_w = 21\,000$ , the ESI/FTMS only looked at about 10% of the chains, and one

might question whether there are additional mechanisms, specific to the high molecular weight chains formed. We have no analytical evidence in support of any additional mechanisms.

Figure 1 is a typical ESI/FTMS spectra of the poly(EA) made at 180 °C using 40 wt % EA on formula. The synthesis was stopped at 90 min and 54% monomer conversion, yielding a 4000 number-average molecular weight polymer with polydispersity of about 2.0. The refractive index detected GPC measurement of this polymer showed a unimodal molecular weight distribution with reasonably narrow polydispersity indicative of consistent polymer chemistry throughout the synthesis. The ESI/FTMS analysis, to about 2500 Da, displays a significant portion of the chains within the molecular weight distribution. Figure 1 shows four families of peaks starting at  $m/z = 423$  continuing to  $m/z = 2326$  with a separation of ~100 Da within each family. We attribute the spacing to EA, which has a molecular formula of  $C_5H_8O_2$  and hence an exact mass of 100.12 Da. The homologous series of EA chains were formed by the same initiating and terminating mechanisms. Table 2 shows the calculated molecular weights of the single sodium ion adducts of the principal chains formed during ethyl acrylate polymerization at higher temperature without added thermal initiator. The  $m/z = 423, 523, 623, \dots$  family of peaks represent chains formed when an ethyl acrylate  $\beta$ -scission radical (formed after a  $\beta$ -scission event) propagates with ethyl acrylate and makes a midchain radical (most likely through intramolecular chain transfer considering the dilute polymer concentration) and subsequently undergoes a  $\beta$ -scission reaction to form a terminally unsaturated macromonomer. The structural formula of such a homologous series of chains is  $\{[CH_2(CO_2X)-CH_2-CH(CO_2X)]-(C_2H_3CO_2X)_n-[CH_2-C(CO_2X)=CH_2]\}Na^+$  where  $X = C_2H_5$  and  $n$  is the number of ethyl acrylate units,  $C_2H_3CO_2X$ , polymerized into the chain. For the largest peak in the expansion plot of Figure 1, at  $m/z = 1124$  Da, the specific structural formula is  $\{[CH_2-$

**Table 2. Possible Molecular Weights of the Single Ionic Species Generated during ESI/FTMS Analysis of Poly(EA) and Poly(nBA)**

poly( <i>n</i> -butyl acrylate)																			
Molecule [I-(nBA) <sub><i>n</i></sub> -T]	<i>n</i> =	1	2	3	4	5	6	7	8	9	10	11	12	13	14	15	16	17	18
xylol initiated H abstraction Mw+Na		513	641	769	898	1026	1154	1282	1410	1538	1666	1794	1922	2050	2178	2306	2435	2563	2691
xylol initiated macromer Mw+Na		525	653	781	910	1038	1166	1294	1422	1550	1678	1806	1934	2062	2190	2318	2447	2575	2703
α scission initiated H abstraction Mw+Na		523	651	779	908	1036	1164	1292	1420	1548	1676	1804	1932	2060	2188	2316	2445	2573	2701
β scission initiated macromer Mw+Na		535	663	791	920	1048	1176	1304	1432	1560	1688	1816	1944	2072	2200	2328	2457	2585	2713
poly(ethyl acrylate)																			
Molecule [I-(EA) <sub><i>n</i></sub> -T]	<i>n</i> =	1	2	3	4	5	6	7	8	9	10	11	12	13	14	15	16	17	18
xylol initiated H abstraction Mw+Na		429	529	629	729	829	929	1030	1130	1230	1330	1430	1530	1630	1730	1830	1930	2030	2130
xylol initiated macromer Mw+Na		441	541	641	741	841	941	1042	1142	1242	1342	1442	1542	1642	1742	1842	1942	2042	2142
α scission initiated H abstraction Mw+Na		411	511	611	711	811	911	1012	1112	1212	1312	1412	1512	1612	1712	1812	1912	2012	2112
β scission initiated macromer Mw+Na		423	523	623	723	823	923	1024	1124	1224	1324	1424	1524	1624	1724	1824	1924	2024	2124

(CO<sub>2</sub>X)-CH<sub>2</sub>-CH(CO<sub>2</sub>X)]-(C<sub>2</sub>H<sub>3</sub>CO<sub>2</sub>X)<sub>8</sub>-[CH<sub>2</sub>C(CO<sub>2</sub>X)=CH<sub>2</sub>]}N<sub>a</sub><sup>+</sup> with molecular formula [C<sub>55</sub>H<sub>88</sub>O<sub>22</sub>]Na<sup>+</sup>. The theoretical isotope distribution agrees well with our experimentally measured isotope envelope. In addition to the family of peaks seen at *m/z* = 423, 523, 623, ..., we detect three other less abundant families of peaks. These lower abundance peaks seen in the expansion plot of Figure 1 are attributed to polymer chains of comparable degrees of polymerization, but different end-group structures. The expansion view in Figure 1 is of the peaks near *m/z* = 1124. The peaks other than *m/z* = 1124 represent chains of similar degree of polymerization but formed through different initiating and/or terminating mechanisms. For example, the *m/z* = 1112 can be assigned to a chain started from an initiating β-scission radical with nine monomer units of propagation and terminated by hydrogen abstraction {[CH<sub>2</sub>-(CO<sub>2</sub>X)-CH<sub>2</sub>-CH(CO<sub>2</sub>X)]-(C<sub>2</sub>H<sub>3</sub>CO<sub>2</sub>X)<sub>9</sub>-H]}N<sub>a</sub><sup>+</sup>. In a similar fashion, the 1130 peak can be assigned to a xylol radical initiated chain with 10 monomer units of propagation and terminated via hydrogen abstraction [C<sub>6</sub>H<sub>4</sub>-(CH<sub>3</sub>)CH<sub>2</sub>-(C<sub>2</sub>H<sub>3</sub>CO<sub>2</sub>X)<sub>10</sub>-H] N<sub>a</sub><sup>+</sup>. The xylol radical is

formed when a growing polymer chain abstracts hydrogen from the xylene solvent molecule. The 1142 peak can be assigned to a xylol radical initiated chain that grew and underwent intramolecular chain transfer and subsequent β-scission to form a macromonomer terminated chain. The structure is [C<sub>6</sub>H<sub>4</sub>(CH<sub>3</sub>)CH<sub>2</sub>-(C<sub>2</sub>H<sub>3</sub>-CO<sub>2</sub>X)<sub>9</sub>-[CH<sub>2</sub>C(CO<sub>2</sub>X)=CH<sub>2</sub>]}N<sub>a</sub><sup>+</sup>. These four clusters of peaks (1112, 1124, 1130, and 1142 Da) represent the four principal types of chains formed and are the result of a 2 × 2 grid of possible chain starting and terminating moieties shown in Table 2 for different degrees of polymerization. While ESI/FTMS is not meant to be strictly quantitative, a rough estimate from Figure 2 would give about 80% of the chains started by β-scission radicals and about 80% of the chains terminated through β-scission to give macromonomer. The β-scission radical initiated chains terminated with macromonomer make up about 60–70% of all the chains formed.

The expansion plot seen in Figure 1 also shows significant peaks at *m/z* = 1074 and 1174 which are indicative of β-scission initiated, macromonomer terminated chains. In the analysis of the EA samples, the

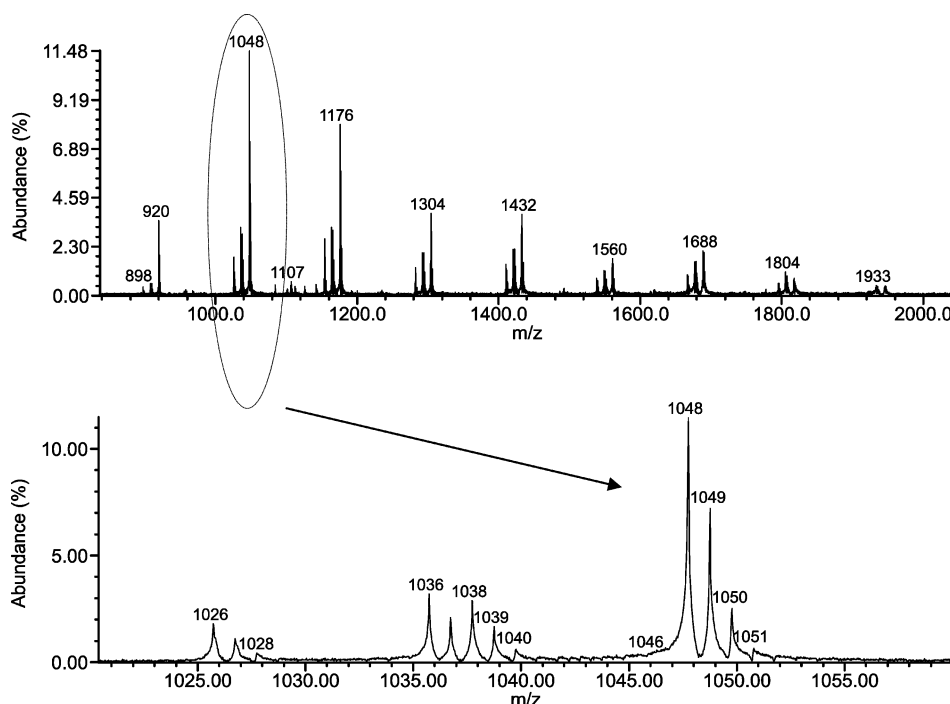


**Figure 2.** ESI/FTMS spectra of poly(*n*-butyl acrylate) sample made by spontaneous polymerization at 180 °C and 40 wt % monomer on solution in the range between 800 and 2000 Da. Also shown is the expanded view of ESI/FTMS results around the peak at 1048 Da. The expanded range is 1020–1060 Da.

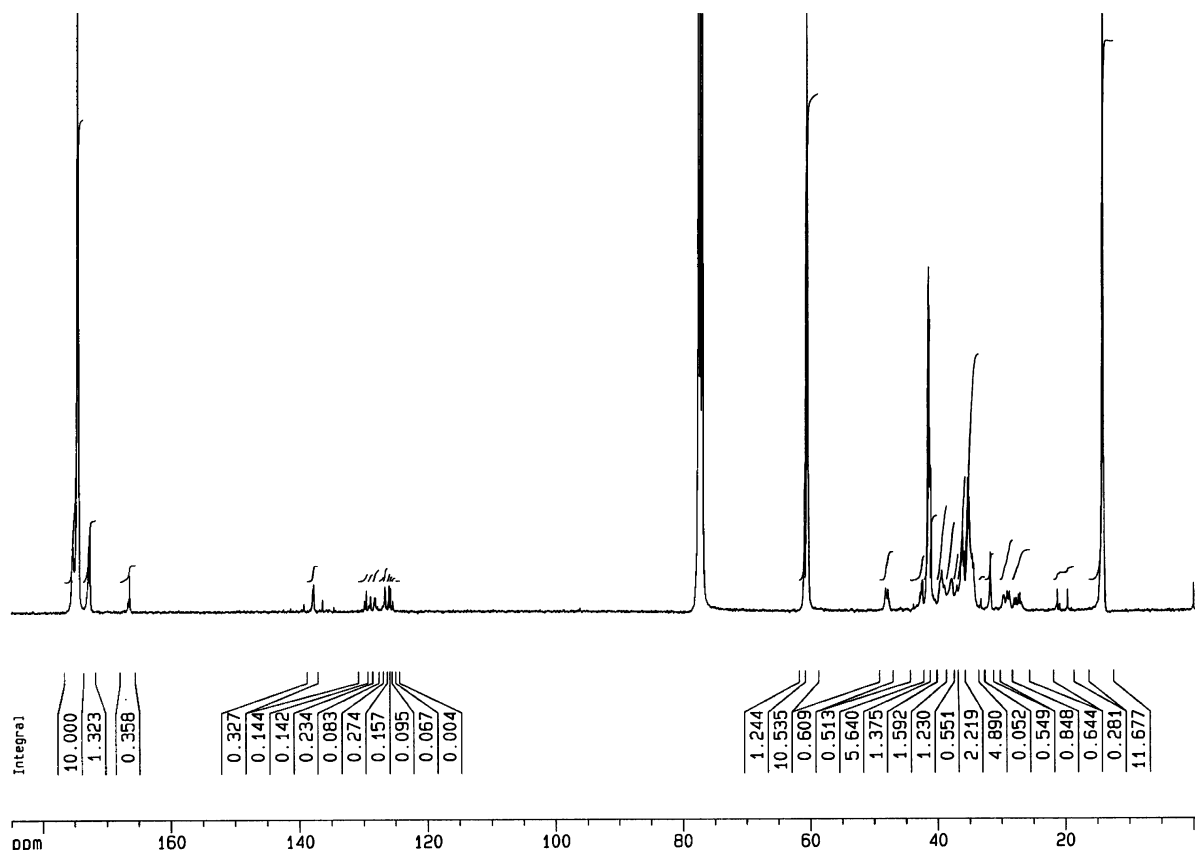


**Figure 3.**  $^{13}\text{C}$  NMR spectra of poly(EA) made at 180 °C and 40 wt % EA in xylene without added thermal initiator.

entire molecular weight distribution was injected in the ESI/FTMS unit at once instead of using a GPC column upstream of the ESI/FTMS unit to inject just the narrow molecular weight fractions eluting at any instant. Injecting the entire molecular weight distribution can lead to the formation and detection of singly, doubly, and triply sodium-attached ionized species in the same spectrum. For example, the  $m/z = 1074$  homologous series represents a doubly charge molecule. Upon close inspection of the isotope patterns, we see that the spacings between  $^{13}\text{C}$  peaks is 0.5 Da instead of the expected 1 Da spacing between  $^{13}\text{C}$  isotopes. The structural formula is given by  $\{[\text{CH}_2(\text{CO}_2\text{X})-\text{CH}_2-\text{CH}(\text{CO}_2\text{X})]-(\text{C}_2\text{H}_3\text{CO}_2\text{X})_{18}-[\text{CH}_2-\text{C}(\text{CO}_2\text{X})=\text{CH}_2]\}-\text{Na}^+\text{Na}^+$  with a molecular weight of  $2 \times 1074 = 2148$  Da. This is a higher molecular weight member of the same  $\beta$ -scission radical initiated, macromonomer terminated homologous series shown in Figure 1 beginning with 423 Da. The 1174 peak in Figure 1 is the  $(\text{C}_2\text{H}_3\text{CO}_2\text{X})_{20}$  version of the above structure. Notice that the chain molecular weight increases by  $\sim 50$  Da ( $1174 - 1124 = 50$ ) for a doubly charged species as opposed to the 100 Da increase for each monomer unit addition. The formation of higher charged states increases the detectable range of molecular weights for FTMS.

Figure 2 and its expansion plot are the ESI/FTMS spectra of poly(nBA) made at 40 wt % nBA on formula and 180 °C to 88% conversion of the nBA at 137 min to yield a 3300 number-average molecular weight polymer with polydispersity of about 2.1. Figure 2 shows a homologous series starting at  $m/z = 920$  and extending to  $m/z = 1816$  in increments of the molecular weight of nBA, 128 Da. Table 2 shows the calculated molecular weights as a function of chain length for the four predominant chain structures seen in the ESI/FTMS

spectra. These chain structures are of the same nature as the EA series. The  $m/z = 920, 1048, 1176, \dots$  series can represent chains formed when a nBA  $\beta$ -scission radical (formed after a  $\beta$ -scission event or via intermolecular chain transfer) propagates with nBA to a point at which it undergoes intramolecular chain transfer to form a terminally unsaturated macromonomer. The structural formula is represented as  $\{[\text{CH}_2(\text{CO}_2\text{Y})-\text{CH}_2-\text{CH}(\text{CO}_2\text{Y})]-(\text{C}_2\text{H}_3\text{CO}_2\text{Y})_n-[\text{CH}_2-\text{C}(\text{CO}_2\text{Y})=\text{CH}_2]\}\text{Na}^+$  where  $\text{Y} = \text{C}_4\text{H}_9$  and  $n$  is the number of saturated nBA units polymerized into the chain. For the largest peak in the expansion plot presented in Figure 2, at 1048 Da, the specific structural formula is given by  $\{[\text{CH}_2(\text{CO}_2\text{Y})-\text{CH}_2-\text{CH}(\text{CO}_2\text{Y})]-(\text{C}_2\text{H}_3\text{CO}_2\text{Y})_5-[\text{CH}_2-\text{C}(\text{CO}_2\text{Y})=\text{CH}_2]\}\text{Na}^+$ . The theoretical and experimental isotope distributions for this oligomer compare reasonably well. As before, the  $m/z = 1036$  peak represents the comparable  $\beta$ -scission radical initiated, hydrogen abstraction terminated chain. The xylol radical initiated, macromonomer terminated chain can be seen at  $m/z = 1038$ . Finally, the xylol radical initiated, hydrogen abstraction terminated chains are seen at  $m/z = 1026$ . These lower abundance chains can be seen more clearly in the expansion plot of Figure 2. The subtle difference between the  $m/z = 1036$  and  $m/z = 1038$  chains are difficult to distinguish, but with the high resolution offered by FTMS these overlapping species can be quantified. The molecular formula for the  $\beta$ -scission radical initiated hydrogen abstraction oligomer chain seen at  $m/z = 1036$  is  $[\text{C}_{55}\text{H}_{96}\text{O}_{16}]\text{Na}^+$  whereas the xylol-initiated macromonomer terminated chain has a molecular formula of  $[\text{C}_{58}\text{H}_{94}\text{O}_{14}]\text{Na}^+$ . These chains differ by a mere 2 Da, and there is overlap between the isotopic envelopes. Fortunately, we can subtract the contribution of the  $^{13}\text{C}$  from the  $\beta$ -scission radical initi-

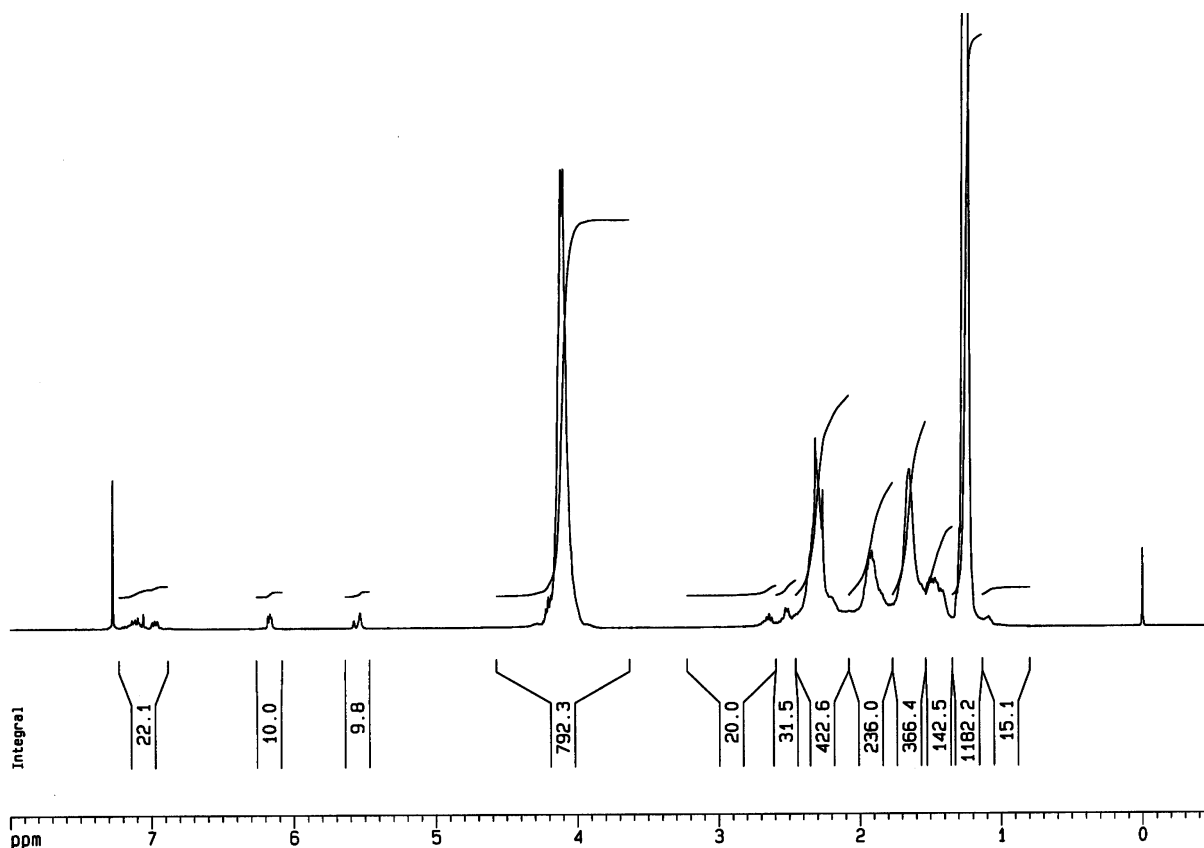


**Figure 4.**  $^1\text{H}$  NMR spectra of poly(EA) made at 180 °C and 40 wt % EA in xylene without added thermal initiator.

ated hydrogen abstraction oligomer to yield the quantity of the xylol-initiated macromonomer terminated species. Using the relative peak areas for the expanded portion of Figure 2, we calculate 60 mol %  $\beta$ -scission initiated, macromonomer terminated species ( $m/z = 1048$ ), 20 mol %  $\beta$ -scission initiated, hydrogen abstraction terminated species ( $m/z = 1036$ ), 10 mol % each of xylol-initiated macromonomer terminated ( $m/z = 1038$ ), and xylol initiated hydrogen abstraction terminated ( $m/z = 1026$ ) species in the polymer distribution. Hence, 80 mol % of the chains are started by  $\beta$ -scission radical, and 70% of the chains are terminated by macromonomer. 20% of the chains are started by xylol radicals, and 30% of the chains are terminated through hydrogen abstraction. These results for nBA are similar to those for EA from Figure 1. Backbiting and  $\beta$ -scission are dominate mechanisms in the acrylate homopolymerization.

**3.3. 1D NMR Analysis.** Lovell's group<sup>20,21</sup> reported on using 1D NMR ( $^{13}\text{C}$  and DEPT) to characterize acrylic polymers, especially nBA polymers and copolymers. In addition, others have used NMR to characterize poly(acrylates) made by other polymerization methods including anionic and group transfer polymerization.<sup>29–31</sup> In this work, poly(EA) and poly(nBA), made at 40 wt % monomer on formula in xylene at 180 °C without thermal initiator, were analyzed using  $^{13}\text{C}$  NMR and  $^1\text{H}$  NMR as shown in Figures 3 and 4 for poly(EA) and  $^{13}\text{C}$  NMR in Figure 5 for poly(nBA). Table 3 shows the peak assignments based on Figure 3 spectra. The backbone methine and methylene peaks are found between 34 and 42 ppm, within which the methine and methylene backbone carbons adjacent to the quaternary carbon branch points are found at 37–40 ppm. The resonance for the quaternary carbon branch points are

found between 48 and 49 ppm. The peaks at 32 and 27.6–30 ppm are assigned to the saturated end group  $\sim\text{CH}_2(\text{CO}_2\text{X})\text{CH}_2$  with  $\text{X} = \text{C}_2\text{H}_5$ . The unknown peak at 42.6 ppm reported in the literature also appears in Figure 5. The  $\text{CH}_3$  on isomeric xylene is assigned to 19.8, 21.0, and 21.5 ppm. The  $=\text{CH}_2$  on the end of macromonomer chains is assigned to 125–128 ppm. The different carbonyl environments are assigned to 165–175 ppm.

The integration of the  $^{13}\text{C}$  NMR spectra can be compared against the computed carbon environments for the  $\beta$ -scission radical initiated chain terminated with macromonomer; the most common chain as determined by ESI/FTMS in this 4000 number-average molecular weight polymer sample. Table 4 shows the computed values for expected integrations as a function of the number of branch points. The integrated area for the branch point carbon at  $\sim 48$  ppm in Figure 3 is 0.61, and this indicates the average number of branch points per chain is about 2.1. In Table 4, the integrated peak areas for the backbone carbon methylene's to methine's increase with the number of branch points. The calculated ratio from Figure 3 of the methylene to methine group areas is 1.2, and this compares well with the same ratio computed in Table 4 when there are two branch points. This ratio will change with the number of branch points as indicated in Table 4. In Figure 3 the absolute value of the integrated peak areas for the backbone carbons are less than expected—the total expected is 22.5 and is measured at 21.0. The predicted peak areas for the total carbonyl peaks, between 166 and 176 ppm, fits well with the experimental data, 11.7 to 11.7. The area of the peak assigned to the carbonyl next to a terminal unsaturation at 166.5 ppm is slightly larger

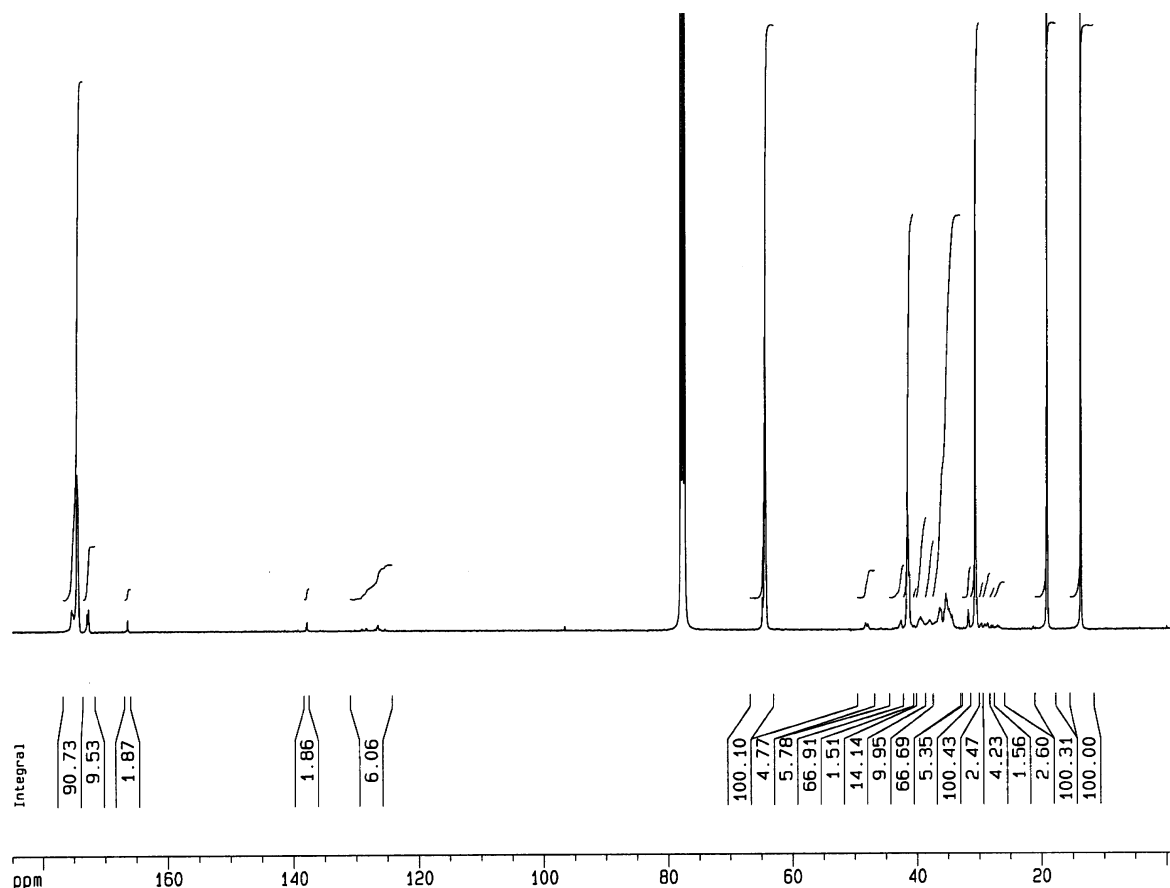


**Figure 5.**  $^{13}\text{C}$  NMR spectra of poly(nBA) made at 180 °C and 40 wt % nBA in xylene without added thermal initiator.

**Table 3. Peak Assignments and Integrated Areas for  $^{13}\text{C}$  NMR Analysis of Poly(EA) Made at 180 °C in Xylene without Added Thermal Initiator**

description	details	peaks
$\text{C}_2\text{H}_5$ in ester linkage	$\text{COOCH}_2\text{CH}_3$ , methyl group $\text{COOCH}_2\text{CH}_3$ methylene group	14.20 60.4–60.9
$\text{CH}_3$ 's on backbone	attached xylene $\text{CH}_3$	19.7–21.3
$\text{CH}_2$ 's in backbone	$\text{CH}_2$ prior to saturated $\text{CH}_2$ on end group $\text{CH}_2$ prior to saturated $\text{CH}_2$ on end group $\text{CH}_2$ saturated end group $\text{CH}_2$ , methylene group in backbone $\text{CH}_2$ , methylene group next to branch point	27.1–27.8 28.0–29.6 31.80 33.2–37.0 37.0–37.9
$\text{CH}$ 's in backbone	methine group in backbone, $-\text{CH}-$ , next to branch point methine group in backbone, $-\text{CH}-$ unassigned peak	37.9–39.4 41.1–41.4 42.50
branch point C's	quaternary carbon's in backbone	47.8–48.3
carbonyl C's	$\text{COOCH}_2\text{CH}_3$ next to terminal unsaturation $\text{COOCH}_2\text{CH}_3$ next to terminal saturation $\text{COOCH}_2\text{CH}_3$ in backbone	166.4–166.7 172.7–172.9 172.9–175.4
aromatic and vinyl C's	aromatic C's C in vinyl at end of chain C in vinyl at end of chain aromatic C's aromatic C's	125.4–126.0 126.7 127.8–128.3 128.9–129.9 137.7–137.9

than that predicted in the model underlying Table 4. As constructed, the carbonyl peak height assigned to terminal unsaturation should not vary with the number of branch points because the mechanisms described herein allow for only one initiation moiety and one terminating moiety per chain. The doublet between 19 and 21 ppm is assigned to the free methyl group on the

xylene attached to the polymer in those chains started by xylene radical. The area of the single carbon present in the terminal unsaturation of the macromonomer, at 126.6 ppm in Figure 3, compares well with the predicted value in Table 4.

In Figure 4, the  $^1\text{H}$  NMR spectra of the poly(EA) sample, the hydrogens on the methyl and methylene

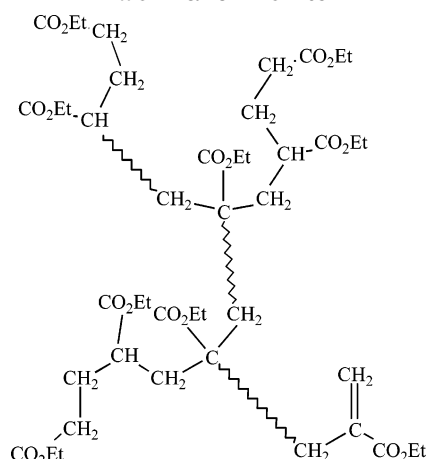
**Table 4. Predicted Peak Integration Areas for a  $\beta$ -Scission Radical Initiated Macromonomer Terminated Poly(EA) Chain as a Function of the Number of Branch Points<sup>a</sup>**

$M_w$ of polymer chain	Number of branch points	$M_w$ in branch points	$M_w$ in straight runs of ea	dp of straight runs	$M_w$ C total	Carbon Balance	quaternary carbons	backbone CH <sub>2</sub> 's	backbone CH's	C's in C=O's	C in CH <sub>2</sub> in ester group	C in CH <sub>3</sub> 's in ester group	C in terminal =CH <sub>2</sub>	Backbone CH <sub>2</sub> 's	CH <sub>2</sub> 's next to quat C	CH <sub>2</sub> 's at end of saturated chain	CH <sub>2</sub> 's next to terminal CH <sub>2</sub> 's	CH <sub>2</sub> 's in bb unaccounted for	Backbone CH's	CH's next to quat C	CH's attached to =CH <sub>2</sub>	CH's in backbone	Carbonyl's	carbonyl's at branch point	carbonyl's @ sat end	carbonyl's next to vinyl group	carbonyl's in backbone
4001	1	300	3701	36.0	2400	0.29	11.96	10.79	11.67	11.67	11.67	0.29	0.88	0.58	0.58	9.92	0.88	0.29	9.63	0.29	0.58	0.29	10.50	0.29	0.58	0.29	10.50
4001	2	600	3401	33.0	2400	0.58	12.25	10.21	11.67	11.67	11.67	0.29	1.75	0.88	0.88	8.75	1.75	0.29	8.17	0.58	0.88	0.29	9.92	0.58	0.88	0.29	9.92
4001	3	900	3101	30.0	2400	0.88	12.55	9.63	11.67	11.67	11.67	0.29	2.63	1.17	1.17	7.59	2.63	0.29	6.71	0.88	1.17	0.29	9.34	0.88	1.17	0.29	9.34
4001	4	1200	2801	27.0	2400	1.17	12.84	9.04	11.67	11.67	11.67	0.29	3.50	1.46	1.46	6.42	3.50	0.29	5.25	1.17	1.46	0.29	8.75	1.17	1.46	0.29	8.75
4001	5	1500	2501	24.0	2400	1.46	13.13	8.46	11.67	11.67	11.67	0.29	4.38	1.75	1.75	5.25	4.38	0.29	3.79	1.46	1.75	0.29	8.17	1.46	1.75	0.29	8.17

<sup>a</sup> The area for the methyl group in the C<sub>2</sub>H<sub>5</sub> ester linkage on the EA molecule is assumed to be 11.67 (per Figure 5) and the molecular weight of the chain is 4001.

groups of the C<sub>2</sub>H<sub>5</sub> ester linkage appear at 1.2 and 4.1 ppm, respectively. Their integrated areas match within experimental error. Brac et al.<sup>29</sup> assign the 1.3–2.0 ppm region to hydrogens on the backbone CH<sub>2</sub>'s and the region from 2 to 2.5 ppm to hydrogens on the backbone CH's. The total integrated area of said backbone hydrogens matches the ester hydrogen peaks within experimental error. Small peaks starting at 2.5 ppm are assigned to the hydrogens on the CH<sub>2</sub> adjacent to the quaternary carbon of the vinylidene end group. This assignment can be confirmed by comparison with MMA dimer, trimer, and tetramer, which have similar vinylidene structure with corresponding CH<sub>2</sub> observed at 2.4–2.5 ppm.<sup>32</sup> The peaks at 2.6–2.7 ppm may be due to stereoisomers. These assignments are based on a chemical shift substitute increment scheme for alkanes and the intensity ratio of well-defined peaks as well as the aid of distortionless enhancement polarization transfer (DEPT) experiments. The DEPT pulse sequence was used to determine the multiplicity of the peaks, i.e., whether the carbon was primary, secondary, tertiary, or quaternary. This method was quite successful in identifying most NMR peaks. The terminal vinylidene structure is highlighted by a pair of resonances at 5.5 and 6.2 ppm due to the different chemical environments for the two hydrogen atoms attached to the same carbon on the terminal unsaturation. Their areas relative to the areas of the hydrogens in the C<sub>2</sub>H<sub>5</sub> ester linkages give vinyl termination levels consistent with those predicted from Table 4 and slightly greater than the ESI/FTMS analysis which indicates about 80% of the chains are vinyl terminated. The peaks at ca. 7.1 ppm are assigned to the hydrogens on xylene internal to the ring, there are 4 of them for xylene, and as measured indicate xylol radical consistent with those determined from the <sup>13</sup>C NMR analysis.

The most likely  $\beta$ -scission initiated, macromonomer terminated chain structure, as indicated by the ESI/FTMS results, is shown in Scheme 3. For the 4000  $M_n$  poly(EA) with 2 branch points, the average run length of monomer would be 11 units with 3 such runs per chain, although the distribution of run lengths need not be even but must total 33. In Scheme 3, the CH<sub>2</sub>(CO<sub>2</sub>Et)-CH<sub>2</sub>CH(CO<sub>2</sub>Et) in the upper left-hand corner represents the  $\beta$ -scission radical initiating species, which can also be written as CH<sub>2</sub>(CO<sub>2</sub>Et)EA. When xylol radical is the initiating species, the CH<sub>2</sub>(CO<sub>2</sub>Et) is replaced by CH<sub>3</sub>–

**Scheme 3.  $\beta$ -Scission Radical Initiated, Macromonomer Terminated Poly(EA) Chain with Two Branch Points<sup>a</sup>**

<sup>a</sup> The wiggly chain represents a run of ethyl acrylate monomer units CH<sub>2</sub>–CH(CO<sub>2</sub>Et). For the 4000 number-average molecular weight poly(EA) with 2 branch points the run would contain 33 EA units. The CH<sub>2</sub>(CO<sub>2</sub>Et)CH<sub>2</sub>CH(CO<sub>2</sub>Et)• represents the  $\beta$ -scission radical initiating species, which can also be written as CH<sub>2</sub>(CO<sub>2</sub>Et)EA. The CH<sub>2</sub>C(CO<sub>2</sub>Et)=CH<sub>2</sub> represents the terminal macromonomer. CH<sub>2</sub>C(CO<sub>2</sub>Et)(CH<sub>2</sub>)CH(CO<sub>2</sub>Et)CH<sub>2</sub>CH<sub>2</sub>(CO<sub>2</sub>Et) represents the branch point.

C<sub>6</sub>H<sub>4</sub>–CH<sub>2</sub>. In the lower right-hand corner of Scheme 3, the CH<sub>2</sub>C(CO<sub>2</sub>Et)CH<sub>2</sub> represents the end group that comprises the terminally unsaturated macromonomer. When hydrogen abstraction terminates the chain the macromonomer is replaced with H. The –CH<sub>2</sub>C(CO<sub>2</sub>Et)–(CH<sub>2</sub>)CH(CO<sub>2</sub>Et)CH<sub>2</sub>CH<sub>2</sub>(CO<sub>2</sub>Et)– depicted twice in Scheme 3 represents the chemical structure of the branch point indicative of the carbon centered radical formed when a growing radical chain intramolecularly abstracts hydrogen from the methine group 3 EA units from the end of the chain. The wrapping or backbiting of the radical preferentially forms a six-membered ring prior to abstraction.

Analysis of Figure 5 for poly(nBA) made at 180 °C and 40% monomer on solution to yield a 3300  $M_n$  polymer give results similar to those for the poly(EA). For the nBA homopolymer the average number of branch points is slightly less at 1.25 per chain—consistent with its lower average molecular weight.

#### 4. Conclusions

The ESI/FTMS and NMR analyses of polymers of EA and nBA made without added thermal initiator at high temperatures to high conversion are consistent with acrylate polymerizations governed by intramolecular chain transfer followed by  $\beta$ -scission to form macromonomers, as shown in Scheme 3. Significant chain transfer to solvent, specifically xylene, was also seen. No strong evidence regarding the nature of the initiating mechanism was found. When a peroxide initiator suitable for such high temperatures was used, the ESI/FTMS analysis showed many chains started with methyl radicals.<sup>5</sup> In this work, no evidence of methyl radicals was found.

**Acknowledgment.** The authors thank Michele J. Bednarek and Recep W. Celikay for performing the NMR and ESI/FTMS analyses. The efforts within are partially supported by DuPont and the National Science Foundation through Grants CTS-9703278 and CST-0216837. Any opinions, findings, and conclusions or recommendations expressed in this work are those of the authors and do not necessarily reflect the views of DuPont or the National Science Foundation.

#### References and Notes

- (1) Cunningham, M. F.; Hutchinson, R. A. In *Handbook of Radical Polymerization*; Matyjaszewski, K., Davis, T. P., Eds.; John Wiley & Sons: Hoboken, NJ, 2002; pp 333–360.
- (2) Adamsons, K.; Blackman, G.; Gregorovich, B.; Lin, L.; Matheson, R. M. *Prog. Org. Coat.* **1997**, *34*, 64–74.
- (3) Slinckx, M.; Henry, N.; Krebs, A.; Uytterhoeven, G. *Prog. Org. Coat.* **2000**, 163–173.
- (4) Haseebuddin, S.; Raju, K. V. S. N.; Yaseen, M. *Prog. Org. Coat.* **1997**, *30*, 25.
- (5) Peck, A. N. F.; Hutchinson, R. A. *Macromolecules* **2004**, *37*, 5944–5951.
- (6) Stobbe, H.; Posnjak, G. *Ann.* **1910**, *371*, 259–86.
- (7) Hui, A. W.; Hamielec, A. E. *J. Appl. Polym. Sci.* **1972**, *16*, 749–769.
- (8) Beigzadeh, D.; Soares, J. B. P.; Hamielec, A. E. *Polym. React. Eng.* **1997**, *5*, 141–180.
- (9) Grady, M. C.; Simonsick, W. J.; Hutchinson, R. A. *Macromol. Symp.* **2002**, *182*, 149–168.
- (10) Hirano, T.; Yamada, B. *Polymer* **2003**, *44*, 347–354.
- (11) Lyons, R. A.; Hutovic, J.; Piton, M. C.; Christie, D. I.; Clay, P. A.; Manders, B. G.; Kable, S. H.; Gilbert, R. G. *Macromolecules* **1996**, *29*, 1918–1927.
- (12) Beuermann, S.; Paquet, D. A., Jr.; McMinn, J. H.; Hutchinson, R. A. *Macromolecules* **1996**, *29*, 4206–4215.
- (13) Wunderlich, W. *Makromol. Chem.* **1976**, *177*, 973–989.
- (14) Scott, G. E.; Senogles, E. J. *Macromol. Sci., Chem.* **1974**, *8*, 753–757.
- (15) Scott, G. E.; Senogles, E. J. *J. Macromol. Sci., Chem.* **1970**, *4*, 1105–1117.
- (16) Subrahmanyam, B.; Baruah, S. D.; Rahman, M.; Baruah, J. N.; Dass, N. N. J. *Polym. Sci., Part A: Polym. Chem.* **1992**, *30*, 2531–2540.
- (17) Van Herk, A. M. *Macromol. Rapid Commun.* **2001**, *22*, 687–689.
- (18) Azukizawa, M.; Yamada, B.; Hill, J. T.; Pomery, P. J. *Macromol. Chem. Phys.* **2000**, *201*, 774–781.
- (19) Yamada, B.; Azukizawa, M.; Yamazoe, H.; Hill, D. J. T.; Pomery, P. J. *Polymer* **2000**, *41*, 5611–5618.
- (20) Chiefari, J.; Jeffrey, J.; Mayadunne, R. T. A.; Moad, G.; Rizzardo, E.; Thang, S. A. *Macromolecules* **1999**, *32*, 7700–7702.
- (21) Ahmad, N. M.; Heatley, F.; Lovell, P. A. *Macromolecules* **1998**, *31*, 2822–2827.
- (22) Lovell, P. A.; Shah, T. H.; Heatley, F. *Polym. Commun.* **1991**, *32*, 98–103.
- (23) Plessis, C.; Arzamendi, G.; Leiza, J. R.; Schoonbrood, H. A. S.; Charmot, D.; Asua, J. M. *Macromolecules* **2000**, *33*, 4–7.
- (24) McCord, E. F.; Shaw, W. H.; Hutchinson, R. A. *Macromolecules* **1997**, *30*, 246–256.
- (25) Plessis, C.; Arzamendi, G.; Leiza, J. R.; Schoonbrood, H. A. S.; Charmot, D.; Asua, J. M. *Macromolecules* **2000**, *33*, 5041–5047.
- (26) Grady, M. C.; Quan, C.; Soroush, M. US Patent Application 60/484,393, 2003.
- (27) Lehrle, R. S.; Shortland, A. *Eur. Polym. J.* **1988**, *24*, 425–429.
- (28) Aaserud, D. J.; Prokai, L.; Simonsick, W. J., Jr. *Anal. Chem.* **1999**, *71*, 4793–4799.
- (29) Brac, A. S.; Hooda, S.; Kumar, R. *J. Polym. Sci.: Part A: Polym. Chem.* **2003**, *41*, 313–326.
- (30) Suchopárek, M.; Spěváček; Masař, B. *Polymer* **1994**, *35*, 3389–3397.
- (31) Kikuchi, H.; Tokumitsu, H.; Seki, H. *Macromolecules* **1993**, *26*, 7326–7332.
- (32) McCord, E. F.; Anton, W. L.; Wilczek, L.; Ittel, S. D.; Nelson, L. T. J.; Raffell, K. D.; Hansen, J. E.; Berge, C. *Macromol. Symp.* **1994**, *86*, 47–64.

MA047528Z